

Electrochemical Reduction of (2,2'-Bipyridine)- and Bis((2-pyridyl)pyrazine)ruthenium(II) Complexes Used as Building Blocks for Supramolecular Species. Redox Series Made of 8, 10, and 12 Redox Steps

Sergio Roffia,^{a,1a} Massimo Marcaccio,^{1a} Carmen Paradisi,^{1a} Francesco Paolucci,^{1a}
Vincenzo Balzani,^{a,1a} Gianfranco Denti,^{1b} Scolastica Serroni,^{1b} and Sebastiano Campagna^{1c}

Dipartimento di Chimica "G. Ciamician", Università di Bologna, Via Selmi 2,
40126 Bologna, Italy, Laboratorio di Chimica Inorganica, Istituto di Chimica Agraria,
Università di Pisa, 56124 Pisa, Italy, and Dipartimento di Chimica Inorganica e Struttura
Molecolare, Università di Messina, 98166 Messina, Italy

Received February 25, 1993

The electrochemical reduction of the $[\text{Ru}(2,3\text{-dpp})_n(\text{bpy})_{3-n}]^{2+}$ complexes ($n = 1-3$), which are extensively used as building blocks for the synthesis of polynuclear compounds, has been investigated at -54°C in DMF solution up to a limit of -3.1 V vs SCE (dpp is the potential bridging ligand bis(2-pyridyl)pyrazine and bpy is 2,2'-bipyridine). For comparison purposes, the electrochemical behavior of the free 2,3-dpp ligand has also been investigated. The results obtained have been discussed and compared with those previously reported for bpy and $\text{Ru}(\text{bpy})_3^{2+}$. Convolutional analysis and simulation of the cyclic voltammetric curves have been performed to obtain the redox potentials in the case of overlapping waves. $[\text{Ru}(2,3\text{-dpp})_3]^{2+}$, $[\text{Ru}(2,3\text{-dpp})_2(\text{bpy})]^{2+}$, and $[\text{Ru}(2,3\text{-dpp})(\text{bpy})_2]^{2+}$ display 12, 10, and 8 reduction steps, respectively, in the potential window examined. The corresponding redox series are thus noticeably more extended than those exhibited by $[\text{Ru}(\text{bpy})_3]^{2+}$ and related complexes not containing bridging-type ligands. The analysis of the genetic diagram which relates the redox potentials observed for 2,3-dpp, $[\text{Ru}(2,3\text{-dpp})_3]^{2+}$, $[\text{Ru}(2,3\text{-dpp})_2(\text{bpy})]^{2+}$, $[\text{Ru}(2,3\text{-dpp})(\text{bpy})_2]^{2+}$, $[\text{Ru}(\text{bpy})_3]^{2+}$, and bpy shows that each redox step in the metal complexes is essentially localized on a specific ligand. A satisfactory assignment of the redox sites has been proposed, and their mutual interactions have been discussed. The results obtained show that in order to arrive at a satisfactory assignment of the redox series for a complex containing redox-active ligands a comparison with the behavior of complexes of the same family is as much instructive as a comparison with the behavior of the free ligands.

Introduction

Assembly of molecular components that possess specific properties is currently matching much attention as a strategy to obtain advanced materials.²⁻⁷ Components with suitable redox potentials and/or excited-state levels are fundamental building blocks for the design of photochemical molecular devices capable of performing important functions such as information storage,⁸ solar energy conversion,^{9,10} and multielectron catalysis.^{10,11}

$\text{Ru}(\text{II})$ complexes of polypyridine-type ligands^{12,13} can be used as building blocks to synthesize redox-active and luminescent supramolecular (polynuclear) metal complexes where electron- and/or energy-transfer processes can be induced by light.^{6,14} A

particularly convenient method to obtain such supramolecular species is that based on the use of bridging ligands (BL) like bis(2-pyridyl)pyrazine (2,3-dpp, Figure 1) to connect metal-containing units.¹⁵ The nonbridging ligands (called terminal ligands, L) present in such supramolecular species are usually 2,2'-bipyridine units (bpy, Figure 1). Using this method, polynuclear $\text{Ru}(\text{II})$ complexes containing 2, 3, 4, 6, 7, 10, 13, and 22 metal atoms, as well as a large numbers of bridging ligands (up to 21) and terminal ligands (up to 24), have been recently obtained.¹⁶

The interpretation of the electrochemical and photophysical behavior of polynuclear metal complexes needs a detailed understanding of the electrochemical and photophysical behavior of each mononuclear component, as shown by previous studies on di- and trinuclear complexes containing other types of bridging ligands.¹⁷⁻³⁴ As one can see from the schematic picture of the tridecanuclear species shown in Figure 2, the essential com-

- (1) (a) University of Bologna. (b) University of Pisa. (c) University of Messina.
- (2) *Molecular Electronic Devices*; Carter, F. L.; Siatkowski, L. E., Wohltjen, H., Eds.; North Holland: Amsterdam, The Netherlands, 1988.
- (3) Kohnke, F. H.; Mathias, J. P.; Stoddart, J. F. *Angew. Chem., Int. Ed. Engl.* **1989**, *28*, 1103.
- (4) Lehn, J. M. *Angew. Chem., Int. Ed. Engl.* **1990**, *29*, 1304.
- (5) *Molecular Electronics*; Lazarev, P. I., Ed.; Kluwer: Dordrecht, The Netherlands, 1991.
- (6) Balzani, V.; Scandola, F. *Supramolecular Photochemistry*; Horwood: Chichester, U.K., 1991.
- (7) Ball, P.; Garwin, L. *Nature* **1992**, *355*, 761.
- (8) Hopfield, J. J.; Onuchic, J. N.; Beratan, D. N. *Science* **1988**, *241*, 817; *J. Phys. Chem.* **1989**, *93*, 6350.
- (9) Amadelli, R.; Argazzi, R.; Bignozzi, C. A.; Scandola, F. *J. Am. Chem. Soc.* **1990**, *112*, 7099. O'Regan, B.; Graetzel, M. *Nature* **1991**, *353*, 737. Graetzel, M. *Comments Inorg. Chem.* **1991**, *12*, 93.
- (10) Wrighton, M. S. *Comments Inorg. Chem.* **1985**, *4*, 269.
- (11) Worl, L. A.; Strouse, G. F.; Younathan, J. N.; Baxter, S. M.; Meyer, T. J. *J. Am. Chem. Soc.* **1990**, *112*, 7571.
- (12) Juris, A.; Balzani, V.; Barigelletti, F.; Campagna, S.; Belser, P.; von Zelewsky, A. *Coord. Chem. Rev.* **1988**, *84*, 85.
- (13) Kalyanasundaram, K. *Photochemistry of Polypyridine and Porphyrin Complexes*; Academic Press: New York, 1992.
- (14) Scandola, F.; Indelli, M. T.; Chiorboli, C.; Bignozzi, C. A. *Top. Curr. Chem.* **1990**, *158*, 73.

- (15) Denti, G.; Serroni, S.; Campagna, S.; Juris, A.; Ciano, M.; Balzani, V. In *Perspective in Coordination Chemistry*; Williams, A. F., Floriani, C., Merbach, A. E., Eds.; Verlag Helvetica Chimica Acta: Basel, Switzerland, 1992; p 153.
- (16) (a) Campagna, S.; Denti, G.; Sabatino, L.; Serroni, S.; Ciano, M.; Balzani, V. *J. Chem. Soc., Chem. Commun.* **1989**, 1500. (b) Denti, G.; Campagna, S.; Sabatino, L.; Serroni, S.; Ciano, M.; Balzani, V. *Inorg. Chem.* **1990**, *29*, 4750. (c) Denti, G.; Campagna, S.; Sabatino, L.; Serroni, S.; Ciano, M.; Balzani, V. In *Photochemical Conversion and Storage of Solar Energy*; Pelizzetti, E., Schiavella, M., Eds.; Kluwer: Dordrecht, The Netherlands, 1991; p. 27. (d) Campagna, S.; Denti, G.; Serroni, S.; Ciano, M.; Balzani, V. *Inorg. Chem.* **1991**, *30*, 3728. (e) Denti, G.; Serroni, S.; Campagna, S.; Ricevuto, V.; Juris, A.; Ciano, M.; Balzani, V. *Inorg. Chim. Acta* **1992**, *198-200*, 507. (f) Denti, G.; Campagna, S.; Serroni, S.; Ciano, M.; Balzani, V. *J. Am. Chem. Soc.* **1992**, *114*, 2944. (g) Campagna, S.; Denti, G.; Serroni, S.; Ciano, M.; Juris, A.; Balzani, V. *Inorg. Chem.* **1992**, *31*, 2982. (h) Serroni, S.; Denti, G.; Campagna, S.; Juris, A.; Ciano, M.; Balzani, V. *Angew. Chem., Int. Ed. Engl.* **1992**, *31*, 1495. (i) Serroni, S.; Denti, G. *Inorg. Chem.* **1992**, *31*, 4251.

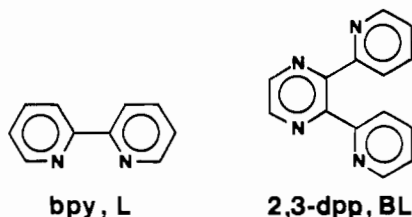


Figure 1. Structural formulas of the bridging ligand (BL) 2,3-bis(2-pyridyl)pyrazine and of the terminal ligand (L) 2,2'-bipyridine.

ponents of the large family of polynuclear compounds containing the 2,3-dpp bridging ligand are the $[\text{Ru}(\mu\text{-BL})_3]^{2+}$, $[\text{Ru}(\mu\text{-BL})_2(\text{L})]^{2+}$, and $[\text{Ru}(\mu\text{-BL})(\text{L})_2]^{2+}$ mononuclear species. As a first step toward the examination of the electrochemical behavior of the polynuclear species, we have carried out a thorough investigation on the $[\text{Ru}(2,3\text{-dpp})_3]^{2+}$, $[\text{Ru}(2,3\text{-dpp})_2(\text{bpy})]^{2+}$, and $[\text{Ru}(2,3\text{-dpp})(\text{bpy})_2]^{2+}$ mononuclear complexes. It will also be shown later that a comparison of the electrochemical behavior of these mononuclear species (and the previously studied $[\text{Ru}(\text{bpy})_3]^{2+}$) is very useful for the identification of the redox sites and for an evaluation of their interactions. For comparison purposes, the behavior of the noncoordinated 2,3-dpp ligand has also been studied. The investigations have been carried out in DMF at -54°C and with scrupulous exclusion of any traces of water and the other proton donors. The results obtained have evidenced extended redox series (i.e., sets of compounds having identical stoichiometric composition and differing only in the overall number of electrons)³⁵ that have been interpreted by means of a genetic diagram which relates the redox potentials observed for the free ligands (2,3-dpp and bpy) and their homo- and heteroleptic Ru complexes.

- (17) (a) Bignozzi, C. A.; Roffia, S.; Scandola, F. *J. Am. Chem. Soc.* **1985**, *107*, 1644. (b) Roffia, S.; Paradisi, C.; Bignozzi, C. A. *J. Electroanal. Chem.* **1986**, *200*, 105. (c) Bignozzi, C. A.; Paradisi, C.; Roffia, S.; Scandola, F. *Inorg. Chem.* **1988**, *27*, 408. (d) Bignozzi, C. A.; Roffia, S.; Chiorboli, C.; Davila, J.; Indelli, M. T.; Scandola, F. *Inorg. Chem.* **1989**, *24*, 4350. (e) Roffia, S.; Casadei, R.; Paolucci, F.; Paradisi, C.; Bignozzi, C. A.; Scandola, F. *J. Electroanal. Chem.* **1991**, *302*, 157. (f) Bignozzi, C. A.; Argazzi, R.; Chiorboli, C.; Roffia, S.; Scandola, F. *Coord. Chem. Rev.* **1991**, *111*, 261. (g) Roffia, S.; Paradisi, C.; Bignozzi, C. A. In Pombeiro, J. L., Ed.; *Molecular Electrochemistry of Inorganic, Bioinorganic and Organometallic Compounds*; Kluwer: Dordrecht, The Netherlands, 1993; p 217. (h) Teixeira, M. G.; Roffia, S.; Bignozzi, C. A.; Paradisi, C.; Paolucci, F. *J. Electroanal. Chem.* **1993**, *345*, 243.
- (18) Krejčík, M.; Vlček, A. A. *Inorg. Chem.* **1992**, *31*, 2390.
- (19) (a) Callahan, R. W.; Brown, G. M.; Meyer, T. J. *Inorg. Chem.* **1975**, *14*, 1443. (b) Goldsby, K. A.; Meyer, T. J. *Inorg. Chem.* **1984**, *23*, 3002. (c) Curtis, J. C.; Bernstein, J. S.; Meyer, T. J. *Inorg. Chem.* **1985**, *24*, 385. (d) Hupp, J. T.; Neyhart, G. A.; Meyer, T. J. *J. Am. Chem. Soc.* **1986**, *108*, 5349. (e) Schanze, K. S.; Neyhart, G. A.; Meyer, T. J. *J. Phys. Chem.* **1986**, *90*, 2182. (f) Tapolsky, G.; Duesing, R.; Meyer, T. J. *J. Phys. Chem.* **1989**, *93*, 3885.
- (20) Sutton, J. E.; Taube, H. *Inorg. Chem.* **1981**, *20*, 3125.
- (21) Gex, J. N.; Brewer, W.; Bergmann, K.; Tait, C. D.; De Armond, M. K.; Hanck, K. W.; Wertz, D. W. *J. Phys. Chem.* **1987**, *91*, 4776.
- (22) (a) Wacholtz, W. F.; Auerbach, R. A.; Schmehl, R. H. *Inorg. Chem.* **1987**, *26*, 2989. (b) Shaw, J. R.; Webb, R. T.; Schmehl, R. H. *J. Am. Chem. Soc.* **1990**, *112*, 1117.
- (23) (a) Sahai, R.; Morgan, L.; Rillema, D. P. *Inorg. Chem.* **1988**, *27*, 3495. (b) Rillema, D. P.; Sahai, R.; Matthews, P.; Edwards, K.; Shaver, R. J. *Inorg. Chem.* **1990**, *29*, 167.
- (24) Katz, N. E.; Creutz, C.; Sutin, N. *Inorg. Chem.* **1988**, *27*, 1687.
- (25) Akasheh, T. S.; El-Ahmed, Z. M. *Chem. Phys. Lett.* **1988**, *152*, 414.
- (26) Zulu, M. M.; Lees, A. J. *Organometallics* **1989**, *8*, 955.
- (27) Bonamira-Soriga, E.; Keder, N. L.; Kaska, W. C. *Inorg. Chem.* **1990**, *29*, 3167.
- (28) Furue, M. *Chem. Lett.* **1990**, 2065.
- (29) (a) Haga, M.; Ano, T.; Kano, K.; Yamabe, S. *Inorg. Chem.* **1991**, *30*, 3843. (b) Onho, T.; Nozaki, K.; Haga, M. *Inorg. Chem.* **1992**, *31*, 4256.
- (30) Curtis, J. C.; Roberts, J. A.; Blackbourn, R. J.; Dong, Y.; Massum, M.; Johnson, C. S.; Hupp, J. T. *Inorg. Chem.* **1991**, *30*, 3856.
- (31) Jacquet, L.; Kirsch-De Mesmaeker, A. *J. Chem. Soc., Faraday Trans.* **1992**, *88*, 2471.
- (32) Pfennig, B. W.; Bocarsly, A. B. *J. Phys. Chem.* **1992**, *96*, 226.
- (33) Lin, R.; Fu, Y.; Brock, C. P.; Guarr, T. F. *Inorg. Chem.* **1992**, *31*, 4346.
- (34) van Diemen, J. H.; Hage, R.; Haasnoot, J. G.; Lempers, H. E. B.; Reedijk, J.; Vos, J. G.; De Cola, L.; Barigelletti, F.; Balzani, V. *Inorg. Chem.* **1992**, *31*, 3518.
- (35) Vlček, A. A. *Coord. Chem. Rev.* **1982**, *43*, 39; *Rev. Chim. Miner.* **1983**, *20*, 612.

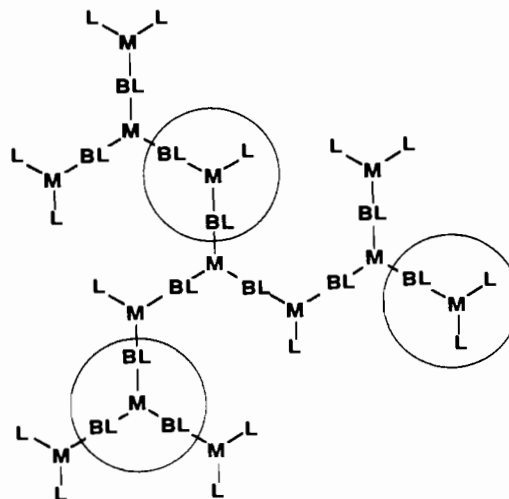


Figure 2. Schematic picture of a tridecanuclear metal complex^{16a} showing the three types of mononuclear units investigated in this work.

Experimental Section

All the materials were reagent grade chemicals. 2,3-Bis(2-pyridyl)pyrazine (2,3-dpp) was prepared according to a literature method.³⁶ The synthesis of the above mentioned complexes has been previously reported.^{15,16} Dry vacuum-distilled *N,N*-dimethylformamide (DMF) was mixed under argon with sodium anthracene and allowed to stand for 5 days in order to remove any traces of water and oxygen, according to the method of Aoyagui and co-workers.³⁷ The solvent was then distilled via a closed system into an electrochemical cell containing the supporting electrolyte and the species under examination.

Cyclic voltammetric experiments were carried out in a single-compartment electrochemical cell of the type described elsewhere,³⁸ utilizing platinum as working and counter electrodes and a silver spiral as quasi-reference electrode. We have verified that its drift was negligible for the time required by an experiment. All the potentials are referred to an aqueous saturated calomel electrode (SCE). They have been determined by adding, at the end of the measurements, $[\text{Ru}(\text{bpy})_3]^{2+}$ as an internal standard. The peak potentials were measured with respect to a $\text{Ru}(\text{bpy})_3^{2+}$ peak, which does not superimpose with those of the species under investigation. The potentials for $\text{Ru}(\text{bpy})_3^{2+}$ referred to SCE, as previously determined,³⁹ are reported in Table I. The cell containing the supporting electrode (C_2H_5)₄NBF₄ was dried under vacuum ($(7-9) \times 10^{-5}$ mbar) at 140°C for 48 h before each experiment. Successively the species under study were introduced, under argon atmosphere, into the cell, which was then kept under the above vacuum conditions for 60 h at 90°C before the distillation of the solvent.

Voltammograms were recorded with an AMEL Model 552 potentiostat controlled by an AMEL Model 568 programmable function generator, an AMEL Model 863 X-Y recorder and a Nicolet Model 3091 digital oscilloscope. The minimization of the uncompensated resistance effect in the voltammetric measurements was achieved by the positive-feedback circuit of the potentiostat. For differential pulse polarography experiments, the equipment used was an AMEL Model 466 polarographic analyzer.

Results and Discussion

The experimental conditions used in this work have allowed us to explore a wide potential window (up to ~ -3.1 V vs SCE). Some of the compounds investigated had previously been studied in a much narrower potential range.^{16,40}

Electrochemical Behavior of Free Ligands. In order to understand the pattern for the ligand-based redox series, one of the main prerequisites is to know the electrochemical behavior of the free ligands. For the free bpy ligand, in a previous study³⁹ performed under the same experimental conditions used in this

(36) Goodwin, H. A.; Lions, F. *J. Am. Chem. Soc.* **1959**, *81*, 6415.

(37) Saji, T.; Yamada, T.; Aoyagui, S. *J. Electroanal. Chem.* **1975**, *61*, 147.

(38) Gas, B.; Klima, J.; Zális, S.; Vlček, A. A. *J. Electroanal. Chem.* **1987**, *222*, 161.

(39) Roffia, S.; Casadei, R.; Paolucci, F.; Paradisi, C.; Bignozzi, C. A.; Scandola, F. *J. Electroanal. Chem.* **1991**, *302*, 157.

Table I. Reduction Potentials in DMF at $-54\text{ }^{\circ}\text{C}$ vs SCE

species	$E_{1/2}/\text{V}$											
	(1)	(2)	(3)	(4)	(5)	(6)	(7)	(8)	(9)	(10)	(11)	(12)
2,3-dpp	-1.93	-2.55	-2.74									
$[\text{Ru}(\text{bpy})_3]^{2+}$ ^a	-1.33	-1.48	-1.70	-2.32	-2.55	-2.85						
$[\text{Ru}(2,3\text{-dpp})(\text{bpy})_2]^{2+}$	-1.04	-1.43	-1.64	-2.06	-2.38	-2.45	-2.65	-2.73				
$[\text{Ru}(2,3\text{-dpp})_2(\text{bpy})]^{2+}$	-0.99	-1.17	-1.58	-1.97	-2.17	-2.40	-2.45	-2.51	-2.57	-2.80		
$[\text{Ru}(2,3\text{-dpp})_3]^{2+}$	-0.94	-1.08	-1.32	-1.93	-2.13	-2.22	-2.59	-2.65	-2.70	-2.73	-2.77	-2.83
bpy ^a	-2.09	-2.69										

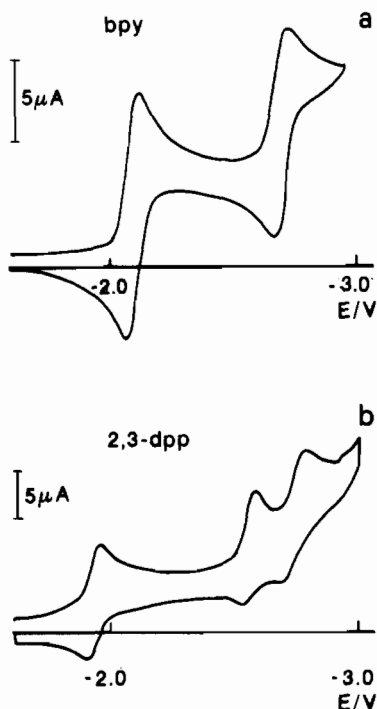
^a Reference 39.

Figure 3. Cyclic voltammogram for 5×10^{-4} M DMF solution of 2,3-dpp (a) and bpy (b) in 0.1 M $(\text{C}_2\text{H}_5)_4\text{NBF}_4$. Working electrode: Pt. Sweep rate: 0.05 V/s. $T = -54\text{ }^{\circ}\text{C}$.

work, two one-electron steps were found, both chemically and electrochemically reversible, with $E_{1/2}$ equal to -2.09 and -2.69 V.

For 2,3-dpp, the data reported in the literature are only relative to the first reduction process due to the restricted potential range investigated.⁴¹ Since we are interested in a much wider potential window, its electrochemical behavior has been re-examined. The cyclic voltammogram (cvc) recorded at low temperature is reported in Figure 3, where the cvc for bpy is also shown for comparison purposes. Three reduction peaks are observed. They are all electrochemically reversible, but while the first is also fully chemically reversible, the second and third peaks present some degree of chemical irreversibility. Each peak corresponds to a one-electron process. By using the usual diagnostic criteria (in particular, by considering that the values of the cathodic current peaks are always in the ratio 1:1:1 in the whole range of sweep rates explored (0.05–50 V/s)), it can be concluded that three electrons are accepted in a sequence by the starting molecule. The possible coupled chemical reactions do not seem to lead to

electroactive species. The $E_{1/2}$ values, obtained by averaging the cathodic and anodic peak potentials, are -1.93 , -2.55 , and -2.74 V.

By comparison of the $E_{1/2}$ value for the first process for the two free ligands, it can be seen that 2,3-dpp is reduced more easily by about 0.2 V with respect to bpy, in agreement with the greater delocalization of its redox orbitals. The two reversible one-electron reduction processes of bpy occur at -2.09 and -2.69 V, and their ΔE (0.60 V) is attributed to the coupling energy of the two electrons in the same redox orbital.³⁵ The first reduction process of 2,3-dpp should mainly concern the pyrazine ring, which is known to be much easier to reduce than pyridine.⁴² The more positive (0.2 V)⁴³ value of the first reduction potential of 2,3-dpp compared with pyrazine can be accounted for by some electron delocalization on the pyridine rings. The second reduction process is displaced toward more negative potentials by ~ 0.6 V, as it happens for other similar ligands (e.g., bpy). This would suggest the coupling of two electrons on the same redox orbital. The lack of theoretical treatments and of experimental data obtained with other techniques prevents the assignment of the third reduction process to a specific orbital or site of the ligand. However this process, as we will see later, is only slightly displaced to more positive potentials upon metal coordination. This would suggest that it involves an orbital mainly localized on the pyridine unit that is not engaged in metal coordination. At any rate, the lack of a specific assignment for the third reduction process of free 2,3-dpp does not affect the discussion that will be reported later concerning the identification of the ligands involved in the various reduction processes of the heteroleptic complexes.

Ligand-Based Redox Series. Before discussion of the ligand-based redox series in the complexes of the $[\text{Ru}(2,3\text{-dpp})_n(\text{bpy})_{3-n}]^{2+}$ family ($n = 0-3$), two important points should be emphasized: (1) 2,3-dpp and bpy have quite different redox properties, as shown by the cvc of the free ligands (Figure 3) and of the two homoleptic complexes (*vide infra*). Since in Ru(II) complexes the ligand–ligand interaction is weak,¹² in the mixed-ligand complexes it should be possible to assign the various redox processes to either 2,3-dpp or bpy. (2) bpy is a symmetric chelating ligand, whereas 2,3-dpp is not symmetric since it uses a pyridine and a (substituted) pyrazine unit for chelation (Figure 1). The nonsymmetric nature of the 2,3-dpp ligands carries two important consequences: (a) For the $[\text{Ru}(2,3\text{-dpp})_2(\text{bpy})]^{2+}$ and $[\text{Ru}(2,3\text{-dpp})_3]^{2+}$ complexes, three and two, respectively, geometrical isomers can exist in principle (Figure 4). (b) Identical chelating ligands may occupy nonequivalent positions in the coordination sphere (see, for example, the two bpy ligands of $[\text{Ru}(2,3\text{-dpp})(\text{bpy})_2]^{2+}$, Figure 4a), and therefore they may experience slightly different ligand–ligand interactions.

$[\text{Ru}(2,3\text{-dpp})(\text{bpy})_2]^{2+}$. On the basis of the behavior of the free ligands, $[\text{Ru}(2,3\text{-dpp})(\text{bpy})_2]^{2+}$ is expected to exchange at least seven electrons (three on 2,3-dpp and two on each bpy ligand).

Figure 5a shows the low-temperature cvc recorded for $v = 0.05$ V/s. As one can see, the curve presents six peaks, the first four corresponding to one-electron diffusion-controlled reversible processes, while each of the last two peaks corresponds to two consecutive one-electron diffusion-controlled reversible processes

- (40) (a) Fuchs, Y.; Lofters, S.; Dieter, T.; Shi, W.; Morgan, R.; Streckas, T. C.; Gafney, H. D.; Baker, A. D. *J. Am. Chem. Soc.* **1987**, *109*, 2691. (b) Ernst, S.; Kasack, V.; Kaim, W. *Inorg. Chem.* **1988**, *27*, 1146. (c) Murphy, W. R.; Brewer, K. J.; Gettcliffe, G.; Petersen, J. D. *Inorg. Chem.* **1989**, *28*, 81. (d) Berger, R. M. *Inorg. Chem.* **1990**, *29*, 1920. (e) Cooper, J. B.; MacQueen, D. B.; Petersen, J. D.; Wertz, D. W. *Inorg. Chem.* **1990**, *29*, 3701. (f) Richter, M. M.; Brewer, K. J. *Inorg. Chem.* **1992**, *31*, 1594. (g) Kalyanasundaram, K.; Graetzel, M.; Nazeeruddin, Md. K. *J. Phys. Chem.* **1992**, *96*, 5865.
- (41) Campagna, S.; Denti, G.; De Rosa, G.; Sabatino, L.; Ciano, M.; Balzani, V. *Inorg. Chem.* **1989**, *28*, 2565.

- (42) Tabner, B. J.; Yandler, J. R. *J. Chem. Soc. A* **1969**, 382.
- (43) Roffia, S.; et al. Unpublished results.

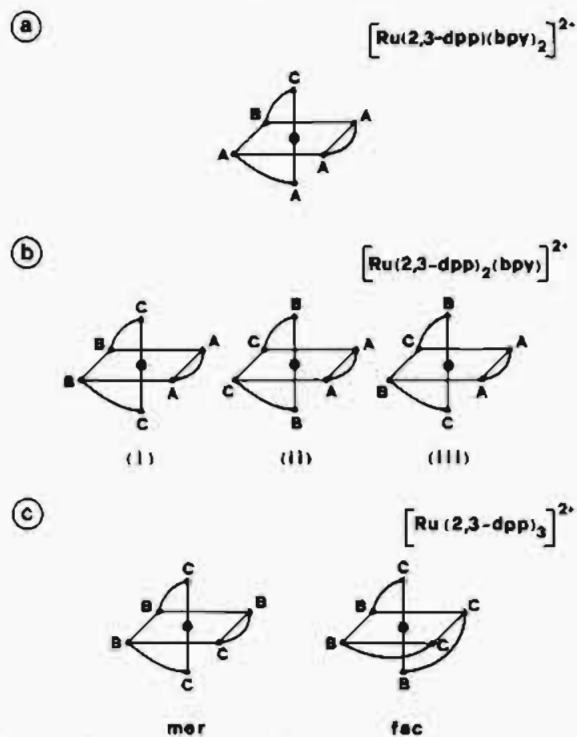


Figure 4. Schematic representation of the possible geometrical isomers for $[\text{Ru}(2,3\text{-dpp})(\text{bpy})_2]^{2+}$ (a), $[\text{Ru}(2,3\text{-dpp})_2(\text{bpy})]^{2+}$ (b), and $[\text{Ru}(2,3\text{-dpp})_3]^{2+}$ (c). B-C and A-A indicate the pyrazine-pyridine and pyridine-pyridine coordinating sites, respectively, of 2,3-dpp and bpy (see Figure 1).

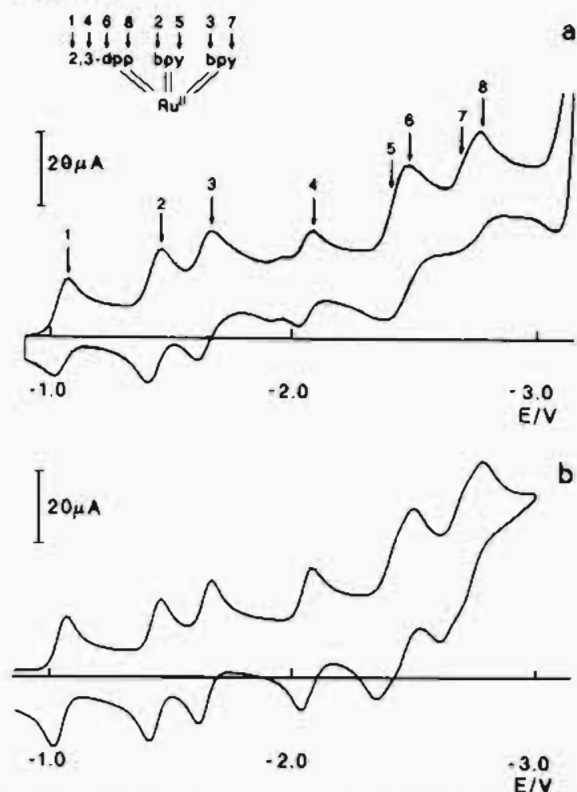


Figure 5. (a) Cyclic voltammogram for a 5×10^{-4} M DMF solution of $[\text{Ru}(2,3\text{-dpp})(\text{bpy})_2]^{2+}$ in 0.1 M $(\text{C}_2\text{H}_5)_4\text{NBF}_4$. Working electrode: Pt. Sweep rate: 0.05 V/s. $T = -54^\circ\text{C}$. (b) Simulated curve for the system and conditions reported in (a) (see text).

with closely spaced standard potentials. Such interpretation is based on the analysis of the morphology and relative heights of the peaks, the scan rate independence of the current function, and the peak potentials of the individual peaks.

The number of electrons exchanged in the individual processes as attributed on the basis of the cvc result is in agreement with

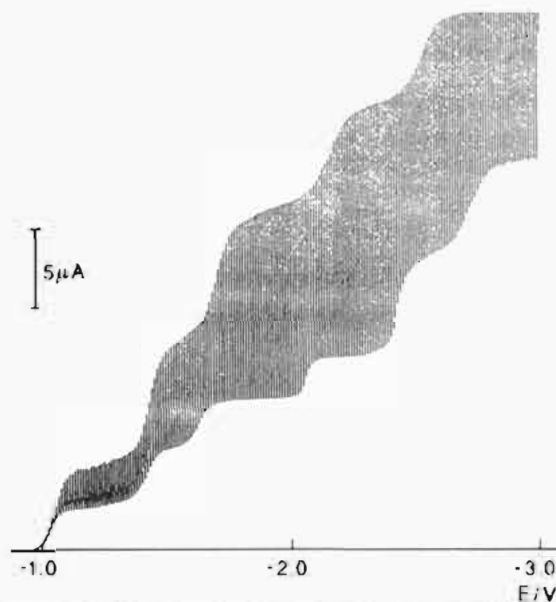


Figure 6. Voltammogram recorded with a platinum electrode with periodical renewal of the diffusion layer for a 5×10^{-4} M DMF solution of $[\text{Ru}(2,3\text{-dpp})(\text{bpy})_2]^{2+}$ in 0.1 M $(\text{C}_2\text{H}_5)_4\text{NBF}_4$. $T = -54^\circ\text{C}$. Renewal time: 3 s.

the data obtained from the voltammogram recorded with a Pt electrode with periodical renewal of the diffusion layer,⁴⁴ where the heights of the waves are in the ratio 1:1:1:1:2:2 (Figure 6). Experiments carried out with the differential pulse polarography technique did not show a significantly greater resolution of the multiplets with respect to the cvc. Therefore we have preferred to examine the cvc curve.

The values of $E_{1/2}$ for the various steps are reported in Table I. For single peaks, $E_{1/2}$ values were directly obtained by averaging the cathodic and anodic peak potentials. For the doublets, the $E_{1/2}$ values were evaluated by convolutive analysis of the cathodic currents according to a procedure described by Ammar and Savéant,⁴⁵ utilizing an algorithm given by Bard and Faulkner for the evaluation of the semi-integral of the current.⁴⁶ In the analysis, the (simulated) extrapolated current curve of the preceding processes was used as base line for each doublet. The contribution to the current from the base solution was taken into account in all the calculations.

The simulated current-potential curve is reported in Figure 5b. As one can see, the agreement between the experimental and simulated curve is satisfactory. The simulation was carried out by extending the method⁴⁷ for a two-step consecutive charge transfer to a multistep charge transfer and considering all the redox steps as one-electron diffusion-controlled reversible processes. The simulation parameters were obtained by a nonlinear regression analysis.⁴⁸

With reference to the identification of the redox sites, a first consideration concerns the extension of the redox series. The comparison between the number of electrons expected on the basis of the behavior of the free ligands (seven) and that experimentally observed (eight) shows that one more electron is exchanged by the complex in the potential window examined. Due to the full reversibility of all steps, this difference can only be accounted for by a reduction concerning the metal center or a further reduction of one of the ligands. The fact that such extra processes are related to the number of 2,3-dpp ligands contained in the complexes (vide infra) suggests that the eighth reduction

(44) Farnia, G.; Roffia, S. *J. Electroanal. Chem.* **1981**, *122*, 347.

(45) Ammar, F.; Savéant, J. M. *J. Electroanal. Chem.* **1973**, *47*, 215.

(46) Bard, A. J.; Faulkner, L. R. *Electrochemical Methods*; Wiley and Sons: New York, 1980; p 239. The algorithm used is eq 6.7.10.

(47) Polcyn, D. S.; Shain, I. *Anal. Chem.* **1966**, *38*, 370.

(48) Niki, K.; Kobayashi, J.; Matsuda, H. *J. Electroanal. Chem.* **1984**, *178*, 333.

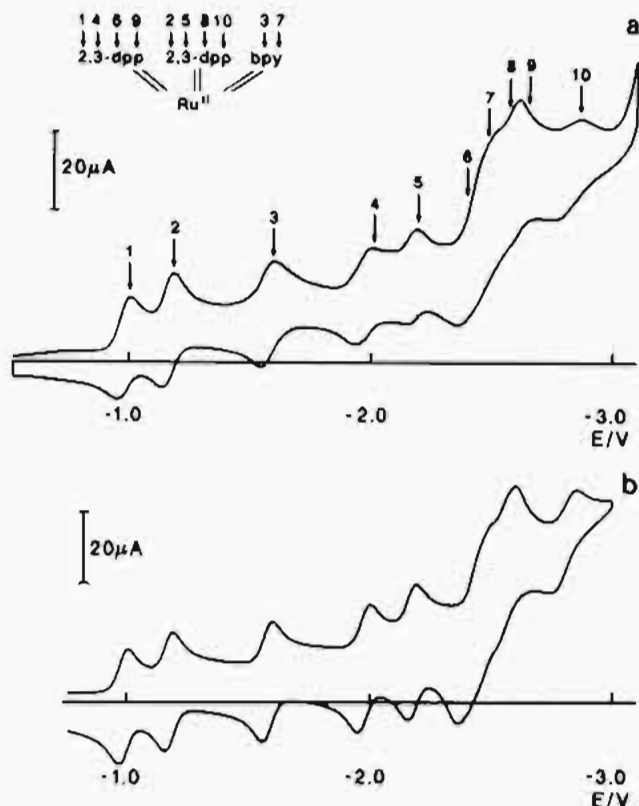


Figure 7. (a) Cyclic voltammogram for a 5×10^{-4} M DMF solution of $[\text{Ru}(\text{2,3-dpp})_2(\text{bpy})]^{2+}$ in 0.1 M $(\text{C}_2\text{H}_5)_4\text{NBF}_4$. Working electrode: Pt. Sweep rate: 0.05 V/s. $T = -54^\circ\text{C}$. (b) Simulated curve for the system and conditions reported in (a) (see text).

process of $[\text{Ru}(\text{2,3-dpp})(\text{bpy})]^{2+}$ concerns the 2,3-dpp ligand. In other words, coordination to the metal increases the ability of 2,3-dpp to accept electrons, either making available another redox orbital or allowing electron pairing in an already available orbital. An analogous behavior observed for 2,2'-bipyrimidine ligated in a dinuclear complex has recently been interpreted in a similar way.¹⁸ In the case of the free 2,3-dpp ligand, EHMO calculations show that the energy separation between the LUMO + 1 and LUMO + 2 orbitals is of the order of magnitude of the electron pairing energy.⁴⁹ Therefore both the above hypotheses are acceptable.

$[\text{Ru}(\text{2,3-dpp})_2(\text{bpy})]^{2+}$. Figure 7a shows the low-temperature cvc recorded for $\nu = 0.05$ V/s. The first five peaks and the last one are reversible, each corresponding to a one-electron process. As to the broad peak which follows the first five ones, an indication of the overall number of electrons exchanged comes from the analysis of the voltammogram obtained with a Pt electrode with periodical renewal of the diffusion layer (Figure 8). The heights of the various successive waves are in the ratio 1:1:1:1:4:1. Therefore, the number of electrons exchanged in correspondence with the broad peak is 4. For this complex, as in the case of the preceding one, the use of differential pulse polarography did not show, for the overlapping waves, a better insight with respect to CV.

Considering all the processes as one-electron diffusion-controlled reversible processes, a simulated curve (calculated according to the above mentioned procedure) has been obtained (Figure 7b). As one can see, the agreement between the experimental and the simulated curve is satisfactory. The $E_{1/2}$ values reported in Table I have been obtained as a mean of the cathodic and anodic peak potentials for the single peaks and by means of the simulation for the broad multielectron peak.

As far as the extension of the redox series is concerned, it can be seen that the number of exchanged electrons exceeds by two

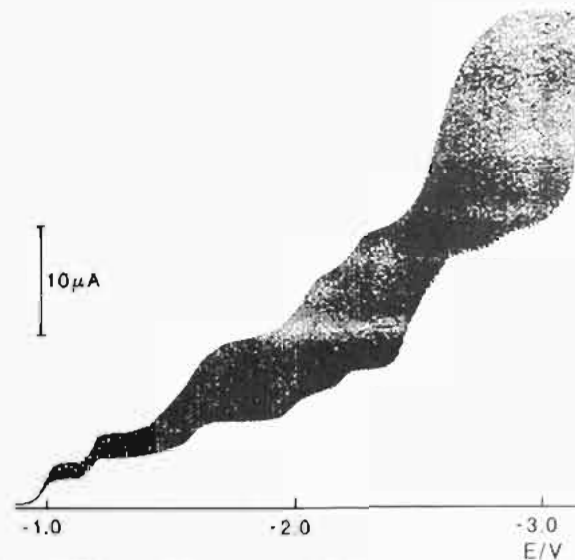


Figure 8. Voltammogram recorded with a platinum electrode with periodical renewal of the diffusion layer for a 5×10^{-4} M DMF solution of $[\text{Ru}(\text{2,3-dpp})_2(\text{bpy})]^{2+}$ in 0.1 M $(\text{C}_2\text{H}_5)_4\text{NBF}_4$. $T = -54^\circ\text{C}$. Renewal time: 3 s.

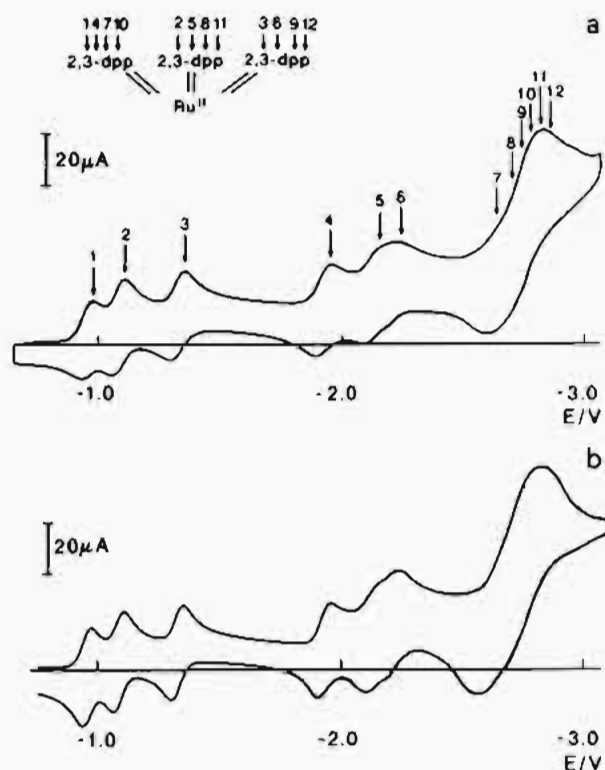


Figure 9. (a) Cyclic voltammogram for a 5×10^{-4} M DMF solution of $[\text{Ru}(\text{2,3-dpp})_3]^{2+}$ in 0.1 M $(\text{C}_2\text{H}_5)_4\text{NBF}_4$. Working electrode: Pt. Sweep rate: 20 V/s. $T = -54^\circ\text{C}$. (b) Simulated curve for the system and conditions reported in (a) (see text).

that expected on the basis of the behavior of the free ligands. This is in line with the preceding hypothesis that 2,3-dpp in the ligated state exchanges one more electron with respect to the free state.

As shown in Figure 4, three different geometrical isomers are possible in principle for $[\text{Ru}(\text{2,3-dpp})_2(\text{bpy})]^{2+}$. The cvc of Figure 7a shows that either only one isomer is present or different isomers exhibit the same electrochemical behavior within the experimental uncertainties.

$[\text{Ru}(\text{2,3-dpp})_3]^{2+}$. Figure 9a shows the low-temperature cvc recorded for 20 V/s. Because of the relatively high sweep rate, the curve has been corrected for the capacitive current by digitally subtracting the corresponding base solution curve stored into the bubble memory of the oscilloscope. The first four peaks correspond to four one-electron diffusion-controlled reversible

(49) De Cola, L.; Barigelli, F. *Gazz. Chim. Ital.* 1988, 118, 477 and unpublished results.

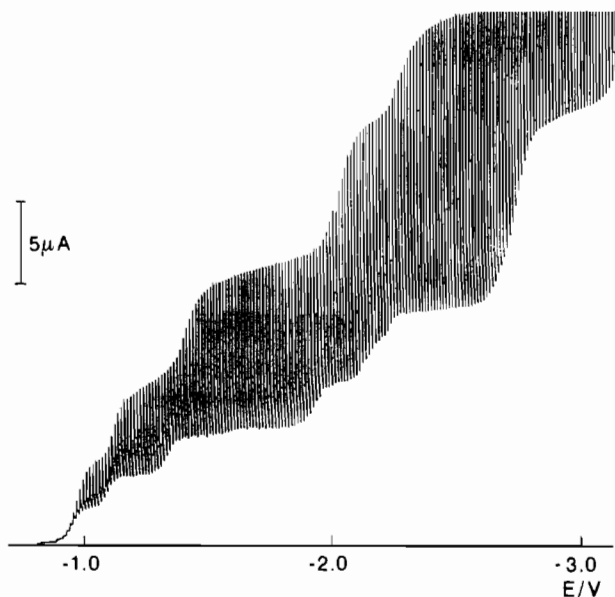


Figure 10. Voltammetric curve recorded with a platinum electrode with periodical renewal of the diffusion layer for a 5×10^{-4} M DMF solution of $[\text{Ru}(2,3\text{-dpp})_3]^{2+}$ in 0.1 M $(\text{C}_2\text{H}_5)_4\text{NBF}_4$. $T = -54^\circ\text{C}$. Renewal time: 3 s.

processes. The fifth peak seems to be composed by two closely spaced one-electron reversible peaks. As to the last broad peak, the charge exchanged during the sweep suggests that it corresponds to six electrons. The number of electrons exchanged in the various processes is in agreement with that obtained by recording a voltammogram with a Pt electrode with periodical renewal of the diffusion layer (Figure 10), where the heights of the waves are in the ratio 1:1:1:1:2:6. Also in the case of this complex differential pulse polarography experiments were carried out in order to see whether a better separation of the overlapping waves was achievable, but the presence of kinetically unstable species made this technique less suitable than CV. On the basis of these results, the simulation of the cvc (Figure 9b) has been carried out under the hypothesis that all the processes are one-electron diffusion-controlled reversible processes.

As one can see from Figure 9, the agreement between the experimental and simulated curves is satisfactory. At lower sweep rates, such as those utilized for recording the cvc for the preceding complexes, the anodic counterpart of the last broad peak is much lower than the cathodic part, which still corresponds to the exchange of six electrons. Due to the multielectron nature of the process, such irreversibility remains unexplained. The $E_{1/2}$ for the various processes, obtained as illustrated before, are reported in Table I.

As far as the extension of the redox series is concerned, the overall number of electrons introduced in the complex (12) is in agreement with the above hypothesis that 2,3-dpp in the ligated state can acquire 4 electrons in sequence.

As shown in Figure 4c, $[\text{Ru}(2,3\text{-dpp})_3]^{2+}$ can exist as two geometrical isomers. ^{99}Ru and ^1H NMR data⁵⁰ indicate a 9:1 ratio of the *mer* and *fac* isomers. In the cvc curve there is no evidence for the presence of two species, presumably because of the large predominance of the *mer* isomer and/or the likely similar behavior of the two isomers.

Identification of the Redox Sites. In order to identify the redox sites, the patterns of the $E_{1/2}$ values for the systems $[\text{Ru}(2,3\text{-dpp})_n(\text{bpy})_{3-n}]^{2+}$ with $n = 0-3$ is compared in Figure 11 with those of the free ligands.

Excluding for the moment the processes not expected on the basis of the behavior of free 2,3-dpp, it can be seen that there is a clear correlation between the redox potentials of the free ligands and those of the corresponding complexes in the sense that, on

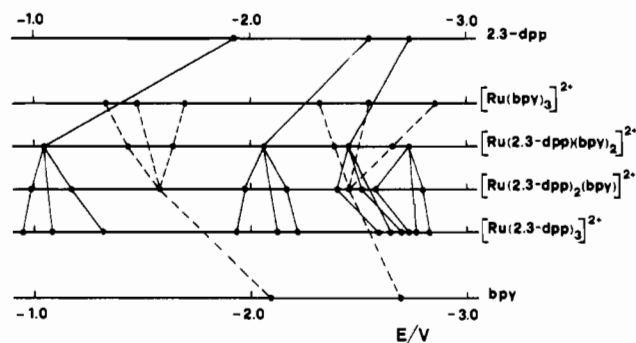


Figure 11. Comparison of the $E_{1/2}$ values (genetic diagram) for the ligands and the complexes $[\text{Ru}(2,3\text{-dpp})_n(\text{bpy})_{3-n}]^{2+}$ ($n = 0-3$) in 0.1 M $(\text{C}_2\text{H}_5)_4\text{NBF}_4/\text{DMF}$. $T = -54^\circ\text{C}$.

going from $[\text{Ru}(\text{bpy})_3]^{2+}$ to $[\text{Ru}(2,3\text{-dpp})_3]^{2+}$ or vice versa, the generation of multiplets of redox processes is observed according to the rules followed by systems containing multiple, mutually and not too strongly interacting redox centers.³⁵

Besides the correlations between the $E_{1/2}$ values of the free ligands and those of the corresponding complexes, the diagram of Figure 11 shows that a correlation also exists for the processes that occur in the coordinated state only, as recently reported for $[(\text{Ru}(\text{bpy})_2)_2(\text{bpm})]^{4+}$ ($\text{bpm} = 2,2'$ -bipyrimidine).¹⁸

It should be pointed out that the correlation established in Figure 11 are unambiguous only for those processes occurring in the same molecule at sufficiently different $E_{1/2}$'s. For other processes the lines connecting the various $E_{1/2}$'s only represent, at this stage of the discussion, correlations between the number of processes which are expected and not expected on the basis of the behavior of free ligands rather than a real succession of occurrence of the processes. Some light on these processes will be thrown by considering the entity of mutual interactions between the redox centers (*vide infra*).

Figures 5a, 7a, and 9a show the assignment proposed on the basis of the correlations shown in the genetic diagram of Figure 11. In this connection and on the basis of the preceding discussion, only the first four, five, and six processes for the complexes $[\text{Ru}(2,3\text{-dpp})(\text{bpy})_2]^{2+}$, $[\text{Ru}(2,3\text{-dpp})_2(\text{bpy})]^{2+}$, and $[\text{Ru}(2,3\text{-dpp})_3]^{2+}$, respectively, are unambiguously localized at the moment.

Redox Sites: Interaction and Localization. The differences among the various $E_{1/2}$ values reported in Figure 11 and in Table I will be now examined in order to obtain information on the mutual interactions among the redox sites and, at the same time, to support the proposed assignment for the localization of the redox sites.

Let us first consider the behavior of the tris complexes. The ligands in the coordinated state are reduced at much more positive potentials compared to the free state, in agreement with the strong stabilization of the redox orbitals produced by the coordination.³⁵ The observed shift is 0.99 and 0.76 V for 2,3-dpp and bpy, respectively. The difference between these two values can reasonably be attributed to a greater ability of 2,3-dpp to donate negative charge to the metal ion.

For both complexes the first six electrons introduced (the only ones observed for the bpy complex) can be grouped in two triplets separated by a potential difference of about 0.6 V, which corresponds to the observed difference between the first and the second peak in the free molecule and which, at least for bpy,³⁵ can be attributed to spin-pairing energy. The separation between successive peaks of triplets are similar but not identical for the two complexes, indicating different interactions between the redox sites. Particularly strong is the difference in the potential separation between the fifth and the sixth peak, which is 90 mV in the 2,3-dpp complex and 300 mV in the bpy complex. This can probably be related to the nonequivalent geometrical situation of the three 2,3-dpp ligands in the *mer* isomer (which is by far the dominant species; see above). In this species, in fact, the three 2,3-dpp ligands have two pyrazines, a pyrazine and a

(50) Predieri, G.; Vignali, C.; Denti, G.; Serroni, S. Work in progress.

pyridine, and two pyridines in the trans positions (Figure 4c). This could imply different ligand–ligand interactions, on successive reduction of the ligands, through the metal orbitals, especially for high electron densities.

The other remarkable feature of $[\text{Ru}(2,3\text{-dpp})_3]^{2+}$ is the presence of a broad six-electron peak. It seems likely that the first three of these six electrons correspond to the third reduction of each 2,3-dpp ligand, already observed in the free ligand (Figure 11). The small stabilization of this process upon coordination (compare with the third reduction potential of the free ligand) and the small separation of the three peaks corresponding to the successive third reduction of each ligand suggest that the third electron enters a 2,3-dpp molecular orbital mainly localized on the noncoordinated pyridine moiety. The small displacement of the successive three peaks suggests that they correspond to occupation of another 2,3-dpp orbital (rather than electron pairing). The fact that such an orbital is not accessible in the free ligand (up to ~ -3.1 V) suggests that it is mainly localized in the coordinating moieties of the ligand.

Let us now consider the mixed-ligand complexes $[\text{Ru}(2,3\text{-dpp})(\text{bpy})_2]^{2+}$ and $[\text{Ru}(2,3\text{-dpp})_2(\text{bpy})]^{2+}$. It will be shown in the following that the redox potentials for the various redox centers can be justified by taking the homoleptic complexes as model compounds for the interaction among the various redox centers and considering the effect deriving from the substitution of bpy for 2,3-dpp ligands.

On the basis of the genetic diagram of Figure 11, the first redox process in the complexes $[\text{Ru}(2,3\text{-dpp})(\text{bpy})_2]^{2+}$ and $[\text{Ru}(2,3\text{-dpp})_2(\text{bpy})]^{2+}$ has been attributed to the reduction of 2,3-dpp. If one also considers, beside these two processes, the first reduction process in $[\text{Ru}(2,3\text{-dpp})_3]^{2+}$, it can be seen that $E_{1/2}$ of the process shifts by about 50 mV toward more negative potentials for each replacement of a 2,3-dpp with a bpy. This can be reasonably ascribed to a lesser delocalization on the whole molecule of the 2,3-dpp redox orbital due to the substitution.

As to the second redox process, in $[\text{Ru}(2,3\text{-dpp})(\text{bpy})_2]^{2+}$ it has been attributed to the reduction of bpy, and its difference with respect to the first one ($\Delta E_{1/2} = -390$ mV) can essentially be explained on the basis of (i) the different reducibility of bpy and 2,3-dpp (the latter being more easily reducible by about 200 mV in the free state; *vide supra*) and (ii) a greater delocalization of the charge introduced by substituting a 2,3-dpp for a bpy. Since the process under discussion concerns a second electron introduced into the complex, a good approximation for evaluating its redox potential is to take $E_{1/2}$ of the second reduction process in $[\text{Ru}(\text{bpy})_3]^{2+}$ and to add 50 mV because of the substitution of a 2,3-dpp in the place of a bpy. The result obtained ($E_{1/2} = -1.43$ V) is coincident with the experimental value. Analogously, the second reduction potential of $[\text{Ru}(2,3\text{-dpp})_2(\text{bpy})]^{2+}$ is, as expected for the second reduction of $[\text{Ru}(2,3\text{-dpp})_3]^{2+}$, decreased by a quantity corresponding to the substitution of a bpy for a 2,3-dpp.

Let us consider the third process. In $[\text{Ru}(2,3\text{-dpp})(\text{bpy})_2]^{2+}$ it has been attributed to the reduction of the second bpy, and $E_{1/2}$ evaluated on this basis agrees well with the experimental observation. As a matter of fact, a good model for this process is the third process in $[\text{Ru}(\text{bpy})_3]^{2+}$ increased by about 50 mV to account for the substitution of a 2,3-dpp for a bpy. The same reasoning can be applied to the third process in $[\text{Ru}(2,3\text{-dpp})_2(\text{bpy})]^{2+}$, which has been attributed to the first reduction of bpy. Since we are dealing with the third electron introduced in the complex, one can take $E_{1/2}$ for the third process in $[\text{Ru}(\text{bpy})_3]^{2+}$ increased by about 100 mV for the substitution of two 2,3-dpp for two bpy's. The value so obtained (-1.60 V) is in good agreement with the experimental value ($E_{1/2} = -1.58$ V). It may be noticed that the separation between the second and third peaks is very close to that observed for $[\text{Ru}(\text{bpy})_3]^{2+}$, which shows that the nonequivalence of the two bpy ligands in $[\text{Ru}(2,3\text{-dpp})(\text{bpy})_2]^{2+}$ caused by the lack of symmetry of the chelating 2,3-dpp ligand is almost negligible.

As far as the fourth process is concerned, for both $[\text{Ru}(2,3\text{-dpp})(\text{bpy})_2]^{2+}$ and $[\text{Ru}(2,3\text{-dpp})_2(\text{bpy})]^{2+}$ the $E_{1/2}$'s are in good agreement with those expected by subtracting from the $E_{1/2}$ value of the fourth process of $[\text{Ru}(2,3\text{-dpp})_3]^{2+}$ 50 and 100 mV for $[\text{Ru}(2,3\text{-dpp})_2(\text{bpy})]^{2+}$ and $[\text{Ru}(2,3\text{-dpp})(\text{bpy})_2]^{2+}$, respectively.

Let us now consider the fifth peak. For $[\text{Ru}(2,3\text{-dpp})(\text{bpy})_2]^{2+}$, it has been attributed to the occurrence of two processes, with rather close standard potentials occurring in bpy and 2,3-dpp, respectively. The following arguments would be in favor of the fact that the reduction of bpy occurs before that of 2,3-dpp. Considering that the process is relative to the introduction of a fifth electron, $E_{1/2}$ expected for the reduction of bpy would be given by $E_{1/2}$ for the fifth process of $[\text{Ru}(\text{bpy})_3]^{2+}$, increased by about 50 mV to account for the substitution in $[\text{Ru}(\text{bpy})_3]^{2+}$ of a 2,3-dpp for a bpy. The resulting $E_{1/2}$ would be -2.50 V, in substantial agreement with the experimental value (-2.38 V).

As far as 2,3-dpp is concerned, the expected $E_{1/2}$ would be that corresponding to the sixth process in $[\text{Ru}(2,3\text{-dpp})_3]^{2+}$ decreased by two contributions, one due to the replacement of two 2,3-dpp with two bpy's and the other due to the fact that we are dealing with a third electron introduced in the same 2,3-dpp molecule and not with a second electron as it is the case in the starting model compound $[\text{Ru}(2,3\text{-dpp})_3]^{2+}$. Considering the behavior of the free ligand, the latter contribution would be equal to about -200 mV. The value thus evaluated is -2.42 V, in good agreement with the experimental value of -2.45 V. Analogous considerations based on the interchange of the two processes (2,3-dpp reduced before bpy) would lead to predicted $E_{1/2}$ values too distant from the observed ones.

With reference to the fifth peak for $[\text{Ru}(2,3\text{-dpp})_2(\text{bpy})]^{2+}$, attributed to the reduction of the second 2,3-dpp, its $E_{1/2}$ agrees well with the value deduced from the fifth $E_{1/2}$ in $[\text{Ru}(2,3\text{-dpp})_3]^{2+}$ decreased by the contribution of the substitution of a bpy for a 2,3-dpp.

The redox potentials corresponding to the various processes of the sixth peak of $[\text{Ru}(2,3\text{-dpp})(\text{bpy})_2]^{2+}$ and the sixth and seventh peaks of $[\text{Ru}(2,3\text{-dpp})_2(\text{bpy})]^{2+}$ are more difficult to justify on the basis of the homoleptic complexes as model compounds for at least two reasons: (i) The electronic interactions become larger in the highly reduced species. (ii) In the case of the seventh electron of both compounds the reference is lacking because $[\text{Ru}(\text{bpy})_3]^{2+}$ exhibits only six reduction processes.

Conclusions

The complexes studied in this work give rise to ligand-based redox series which are typical of systems with multiple, weakly interacting redox centers. The observed redox series formed by 8, 10, and 12 one-electron steps for $[\text{Ru}(2,3\text{-dpp})(\text{bpy})_2]^{2+}$, $[\text{Ru}(2,3\text{-dpp})_2(\text{bpy})]^{2+}$, and $[\text{Ru}(2,3\text{-dpp})_3]^{2+}$, respectively, are considerably more extended than those previously reported for complexes of the polypyridine family.

The analysis of a genetic diagram displaying the change of redox potentials for the various processes for the systems $[\text{Ru}(2,3\text{-dpp})_n(\text{bpy})_{3-n}]^{2+}$ ($n = 0-3$) has allowed us to propose a satisfactory assignment for the localization of the redox sites and to obtain information on the extent of their mutual interaction. The results obtained have also shown that the extension of the redox series cannot be judged only on the basis of the behavior of the unligated centers since other redox orbitals of the ligands can become accessible upon coordination.

The detailed knowledge of the electrochemical behavior of the $[\text{Ru}(2,3\text{-dpp})_n(\text{bpy})_{3-n}]^{2+}$ building blocks will now allow us to investigate and interpret the very complicated electrochemical behavior of oligonuclear complexes of this family.

Acknowledgment. We thank Mr. L. Minghetti for technical assistance. This work was supported by the Ministero dell'Università e della Ricerca Scientifica e Tecnologica and by the Consiglio Nazionale delle Ricerche.